JOURNAL OF CATALYSIS **176,** 25–34 (1998)
ARTICLE NO. CA981992

Effects of the Thermal Stability and the Fine Structure Changes of Strontium Hydroxyapatites Ion-Exchanged with Lead on Methane Oxidation in the Presence and Absence of Tetrachloromethane

Shigeru Sugiyama,*[,1] Yoshimasa Iguchi,* Hitoshi Nishioka,* Toshimitsu Minami,* Toshihiro Moriga,* Hiromu Hayashi,* and John B. Moffat†

*Department of Chemical Science and Technology, Faculty of Engineering, The University of Tokushima, Minamijosanjima, Tokushima 770-8506, Japan; and †Department of Chemistry and the Guelph-Waterloo Centre for Graduate Work in Chemistry, University of Waterloo, Waterloo, Ontario N2L 3G1, Canada

Received March 4, 1997; revised December 12, 1997; accepted December 15, 1997

The oxidation of methane has been investigated in the presence and absence of tetrachloromethane (TCM) on strontium hydroxyapatite with (SrPbHAp) and without (SrHAp) ion-exchanged lead. In the absence of TCM at 873 K, the introduction of lead to strontium hydroxyapatite resulted in a substantial increase in the selectivity to C_2 hydrocarbons and an increase in the conversion of methane and specific activities. In the presence of TCM, the conversion of methane and the selectivity to C_2 compounds decreased with increasing time-on-stream while that to carbon monoxide increased. However, the change in the specific activities with time-on-stream is dependent upon the composition of the catalysts. Some SrPbHAp catalysts showed evidence of transformation from apatites to the corresponding phosphates at temperatures greater than 873 K. At 773 K, at which temperature the aforementioned hydroxyapatites are relatively stable, no formation of C_2 compounds was observed in the absence of TCM, and the conversion of methane and the specific activities (with the exception of SrPb26HAp at 0.5 h on-stream) increased with the lead content of the catalysts. On introduction of TCM, the selectivities to CH_3Cl and CO_2 increased and decreased, respectively, on both SrHAp and SrPbHAp catalysts. The results of extended X-ray absorption fine structure (EXAFS) spectroscopic measurements suggest that the catalytic properties of SrPbHAp at 773 K in the absence of TCM are related to the nearest-neighbor distances of the Pb–O bond rather than those of the Sr–O bond.

INTRODUCTION

In the oxidative coupling of methane on heterogeneous catalysts the introduction of solid- and/or gas-phase additives frequently leads to beneficial increases in conversion of methane and selectivity to C_2 hydrocarbons. Although compounds of lead have been shown to be appropriate catalysts for the aforementioned process (1–22), many of these suffer from the relatively high volatibility of lead (23). While the phosphate (24, 25) and sulphate (24) of lead are less volatile the conversions observed with these compounds are disadvantageously low. Recently, calcium hydroxyapatite ion-exchanged with lead has been shown to generate, with little or no deactivation, C_2 selectivities greater than 80% and conversions of 10% at 973 K (26, 27) while the same compound, in the absence of lead produces the oxides of carbon (26, 28).

As a gas-phase additive, tetrachloromethane (TCM) has been extensively studied in our laboratories (29). The addition of a small quantity of TCM into the feedstream for methane conversion generally leads to an increase in the conversion of methane and the selectivity to ethylene together with a decrease in that to ethane concomitant with a reduction in carbon oxides (29). These advantageous effects have been attributed to the interaction of TCM with the catalysts and the introduction of chlorine species on and in the catalysts as the corresponding chlorides or oxychlorides (29). However, the introduction of TCM into the feedstream over calcium (30–32) and strontium (33, 34) hydroxyapatites produces an increase in the selectivity to CO without the formation of coupling products. In these catalyst systems, it has been pointed out that the corresponding chlorapatite formed during the oxidation in the presence of TCM appears to contribute to the effects of the gas phase additive (30–34).

Among a wide variety of hydroxyapatites (35), calcium hydroxyapatite [$Ca_{10-x}(HPO_4)_x(PO_4)_{6-x}(OH)_{2-x}$; $(0 \le x \le 1)$] has been shown to possess acidic or basic properties which are dependent upon its composition (36–41). The activation of methane has been attributed to basic sites which are present on many of the catalysts that are active in the methane conversion process (1, 4, 9, 23). Because

[1] To whom correspondence should be addressed. Tel.: (+81-886) 567432. Fax: (+81-886) 557025. E-mail: sugiyama@chem.tokushima-u.ac.jp.

0021-9517/98 $25.00

the conversion of methane on strontium hydroxyapatite is higher than that on its calcium analogue (30–34, 42), an observation which has been attributed to differences in the cationic electronegativities of the catalysts (29), it is of interest to examine the effect of the introduction of lead and TCM with the former catalyst on the oxidation process.

In the present study, the thermal stabilities of strontium hydroxyapatite and those ion-exchanged with lead and the catalytic activities for the oxidation of methane in the presence and absence of TCM are reported. X-ray diffraction (XRD) and X-ray photoelectron spectroscopy (XPS) of the catalysts prior to and after use in the oxidation process is employed for characterization purposes and the results from extended X-ray absorption fine structure (EXAFS) spectroscopy provide information on the nearest-neighbor distances of Sr–O and Pb–O in the catalysts.

EXPERIMENTAL

Catalyst Preparation

Strontium hydroxyapatite was prepared from $Sr(NO_3)_2$ (Wako Pure Chemicals, Osaka) and $(NH_4)_2HPO_4$ (Wako) according to the procedure of Matsumura *et al.* (42). The resulting solid was calcined at 773 K for 3 h after drying in air at 373 K overnight. Lead cation was ion-exchanged into the hydroxyapatite by stirring the apatite sample (20 g) in 150 or 200 mL of aqueous solution of $Pb(NO_3)_2$ (Wako) at room temperature (43). Undoped catalyst (denoted as SrHAp) was treated in the same manner but without the addition of lead nitrate. Additional details can be found in Table 1. After it was washed with water and dried at 373 K overnight, the sample after calcination at 773 K for 3 h was referred to as the "fresh catalyst." All catalysts were sieved to particle sizes of 1.70–0.85 mm. The concentrations of Sr, Pb, and P in each catalyst were measured in aqueous HNO_3 solutions with inductively coupled plasma (ICP) spectrometry. The ion-exchanged catalysts are denoted as SrPb*xx*HAp, with *xx* equal to 100Pb/Sr (atomic ratio). The BET surface areas, apparent densities and the atomic ratios of Sr/P and Pb/P of each catalyst are summarized in Table 1.

Apparatus and Procedure

The catalytic experiments were performed in a fixed-bed continuous-flow quartz reactor operated at atmospheric pressure. The reactor consisted of a quartz tube, 9 mm i.d. and 35 mm in length, sealed at each end to 4 mm i.d. quartz tubes to produce a total length of 25 cm. The catalyst charge was held in place in the enlarged portion of the reactor by two quartz wool plugs (30). Prior to reaction the catalyst was calcined *in situ* in an oxygen flow (25 mL/min) at a given temperature (see text) for 1 h. The reaction conditions were as follows: $W = 0.5$ g, $F = 30$ mL/min, $T = 873$ or 773 K, $P(CH_4) = 28.7$ kPa, $P(O_2) = 4.1$ kPa, and $P(TCM) = 0$ or 0.17 kPa; balance to atmospheric pressure was provided by helium.

Analysis and Characterization

The reactants and products were analyzed with an on-stream gas chromatograph (Shimadzu GC-8APT) equipped with a TC detector and integrator (Shimadzu C-R6A). The columns used in the present study and the method employed in the calculation of conversions and selectivities have been described previously (30). Specific activities (mmol/s m^2) at 0.5 and 6 h on-stream were calculated from the conversions and surface areas of the fresh catalysts and those measured after 6 h on-stream, respectively.

TABLE 1

Preparation Conditions, Composition, Surface Area, and Apparent Density of Fresh SrHAp and SrPbHAp Catalysts

Catalyst	Pb conc.[a]	Time[b]	Sr/P[c]	Pb/P[c]	Pb/Sr[c]	SA[d]	AD[e]
SrHAp	0 mmol/150 mL	24	1.62 (1.66)	0 (0)	0 (0)	65.6	0.31
SrPb11HAp	13.5 mmol/150 mL	68	1.42 (1.55)	0.16 (0.17)	0.11 (0.11)	55.2	0.41
SrPb26HAp	101 mmol/250 mL	24	1.50 (1.40)	0.40 (0.37)	0.26 (0.26)	22.3	0.60
SrPb33HAp	33.8 mmol/150 mL	24	1.21 (1.31)	0.40 (0.38)	0.33 (0.29)	46.7	0.37
SrPb71HAp	67.6 mmol/150 mL	68	1.09 (1.04)	0.78 (0.71)	0.71 (0.68)	17.3	0.64

[a] Initial concentration of lead ion in ion-exchange solution.
[b] Duration of ion-exchange at room temperature (h).
[c] Atomic ratio. Values in parentheses show the ratios after calcination for 3 h at 973 K.
[d] BET surface area (m^2/g).
[e] Apparent density (g/cm^3).

The surface areas of the catalysts were calculated from adsorption isotherms obtained with a conventional BET nitrogen adsorption apparatus (Shibata P-700).

X-ray photoelectron spectroscopy (XPS; Shimadzu ESCA-1000AX) used monochromatized Mg$K\alpha$ radiation. The binding energies were corrected using 285 eV for C 1 s as an internal standard. Argon-ion etching of the catalyst was carried out at 2 kV for 1 min with a sputtering rate estimated at ca. 20 Å/min for SiO_2.

Powder X-ray diffraction (XRD) patterns were recorded with a Rigaku RINT 2500X diffractometer, using monochromatized Cu$K\alpha$ radiation. Patterns were recorded over the 2θ range of 5–60°.

The concentrations of Sr, Pb, and P and Cl when present, in each catalyst were determined in aqueous HNO_3 solutions by ICP (SPS-1700, Seiko) or ion chromatography (Shimadzu PIA-1000).

EXAFS near the Sr K- and Pb L_3-edges were measured (2.5 GeV) at the National Laboratory for High-Energy Physics with a storage ring current of ca. 320 mA. The X-rays were monochromatized with channel-cut Si(311) crystals, and the absorption spectra were observed using ionization chambers in a transmission mode. The sample diluted with BN was compressed into a disc 13 mm in diameter. The photon energy was scanned in the range 15.8–17.1 keV for the Sr K-edge and 12.5–14.1 keV for the Pb L_3-edge. Following the standard procedure, we extracted the EXAFS interference function $\chi(k)$ from the absorption spectra. The radial structure functions $\phi(r)$ were obtained from the Fourier transforms of $k^3\chi(k)$. The backscattering amplitude and the phase shift function calculated by McKale *et al.* (44) were used. For the curve-fitting, the range of interest for $\phi(r)$ was filtered with a Hamming window function, and transformed back to k space, $\chi'(k)$. Curve-fitting calculations for $\chi'(k)$ (45) were performed over k ranges of 3–12 and 3–8 $Å^{-1}$ for Sr and Pb, respectively.

RESULTS AND DISCUSSION

Thermal Stability of SrPbHAp Catalysts

Although it has been reported that SrHAp of various Sr/P ratios is stable at temperatures less than 873 K (33), the introduction of lead through ion-exchange appears to reduce the thermal stability at 873 K (Fig. 1). Phosphates of strontium [JCPDS 24-1008] and lead [JCPDS 22-0668] were detected in the XRD patterns, except for those of SrHAp and SrPb26HAp, together with the corresponding hydroxyapatites [JCPDS 33-1348 and 8-0259, respectively]. To illustrate both compositional and temperature effects on the process in which hydroxyapatite is converted to the corresponding phosphate the relative intensities, I_{PO}/I_{Ap}, are summarized in Table 2, where I_{PO} represents the summation of the intensities of the 29.6 and 28.9° signals, both assigned to (015) planes of $Sr_3(PO_4)_2$ and $Pb_3(PO_4)_2$, respectively, while I_{AP} represents the intensities of the signals appearing at 30.5 and 30.1°, the former of which is assigned to the (211) and (112) planes of $Sr_{10}(PO_4)_6(OH)_2$ (overlapping), and the latter to the (211) plane of $Pb_{10}(PO_4)_6(OH)_2$, respectively. As reported previously (33), the conversion of the hydroxyapatite to the phosphate occurs at temperatures as low as 973 K for SrHAp. Although SrPb26HAp appears to be more stable than SrHAp, the remaining catalysts are apparently thermally unstable and are converted to the

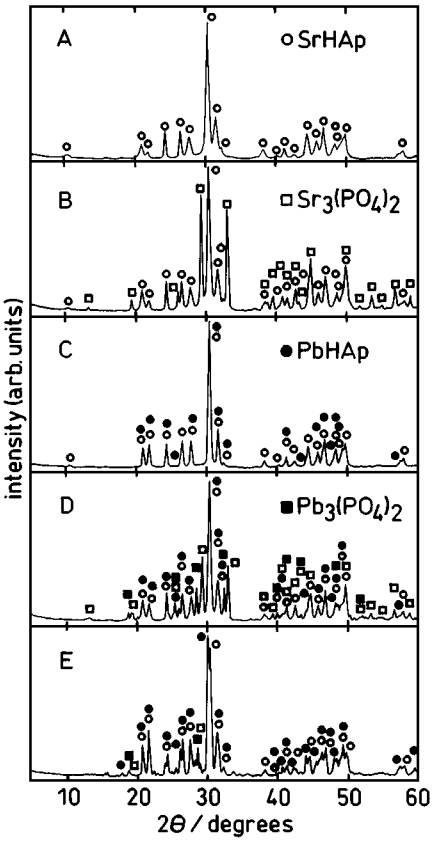

FIG. 1. XRD patterns of fresh catalysts calcined at 873 K for 3 h: (A) SrHAp; (B) SrPb11HAp; (C) SrPb26HAp; (D) SrPb33HAp; (E) SrPb71HAp.

TABLE 2

Relative XRD Intensities of I_{PO}/I_{Ap}[a] in SrHAp and Various SrPbHAp Pretreated at Different Temperatures for 3 h

Temp.[b]/ K	Catalyst				
	SrHAp	SrPb11HAp	SrPb26HAp	SrPb33HAp	SrPb71HAp
773	0	0	0	0.18	0.13
873	0	0.52	0	0.42	0.15
973	0.38	1.69	0.03	2.06	0.43

[a] I_{PO}, $\sum$(intensity of $Sr_3(PO_4)_2$ at $2\theta = 29.6°$ and that of $Pb_3(PO_4)_2$ at $2\theta = 28.9°$). I_{AP}, $\sum$ (intensity of $Sr_{10}(PO_4)_6(OH)_2$ at $2\theta = 30.5°$ and that of $Pb_{10}(PO_4)_6(OH)_2$ at $2\theta = 30.1°$).

[b] Pretreatment temperature.

corresponding phosphate at 973 K. Although loss of phosphate groups is not uncommon at high temperatures with a variety of phosphates, little or no evidence for such losses was found with the present solids at least at 973 K (Table 1). These results suggest that the thermal stability of SrHAp, while at least in part related to the concentration of ion-exchanged lead, is evidently also dependent on additional factors. The source of the thermal stability of SrPb26HAp relative to that of SrHAp is, at this time, unclear, and further relevant experiments are in progress.

Oxidation of Methane on SrHAp and SrPbHAp

In order to compare the catalytic activities of SrPbHAp with those previously reported for SrHAp (34), the oxidation of methane on SrPbHAp has been examined under the same reaction conditions employed in the previous study (34), in which the reaction and pretreatment temperatures were held at 873 K. As reported previously (34) with SrHAp and in the absence of TCM no C_{2+} hydrocarbons are found in the product and the carbon oxides are predominantly CO while CH_3Cl is formed in the presence of TCM at 6 h on-stream (Fig. 2). On introduction of lead the conversion of methane in the absence of TCM increased twofold and significant selectivities to C_{2+} hydrocarbons, particularly for C_2H_6, were measured while CO vanished from the product stream, all of which showed relatively little change on increase of the lead content. As noted above (see Table 2) a portion of each of the catalysts, with the exception of SrPb26HAp, is converted to the corresponding phosphate at 873 K. With the exception of SrPb33Hap the surface areas of the fresh catalysts decreased with the addition of lead (Table 1). The surface areas of each composition decreased during 6 h on-stream at 773 and 873 K with the largest decrease evident at the higher temperature (Table 3). Thus the specific activities at either temperature were generally found to increase after 6 h on-stream in large part as a result of the aforementioned decreases in surface area (Table 3). The observations from the methane conversion process in the absence of TCM appear to be largely dependent upon the presence of the apatites as opposed to the phosphates.

Upon addition of TCM to the feedstream the conversion of methane on the various compositions decreased with increasing time-on-stream while the specific activities after 6 h on-stream reflected the generally substantial decreases in surface areas during the oxidation process. It should be noted that the conversions, specific activities, and selectivities at 0.5 h on-stream in the presence of TCM with the leaded samples were similar to those found in the absence of TCM. However at 6 h on-stream little or no hydrocarbons were observed with those three samples containing the higher concentrations of lead and the product was largely composed of CO and CH_3Cl.

XRD patterns of catalysts previously employed in the oxidation in the presence of TCM (Fig. 3) show that all

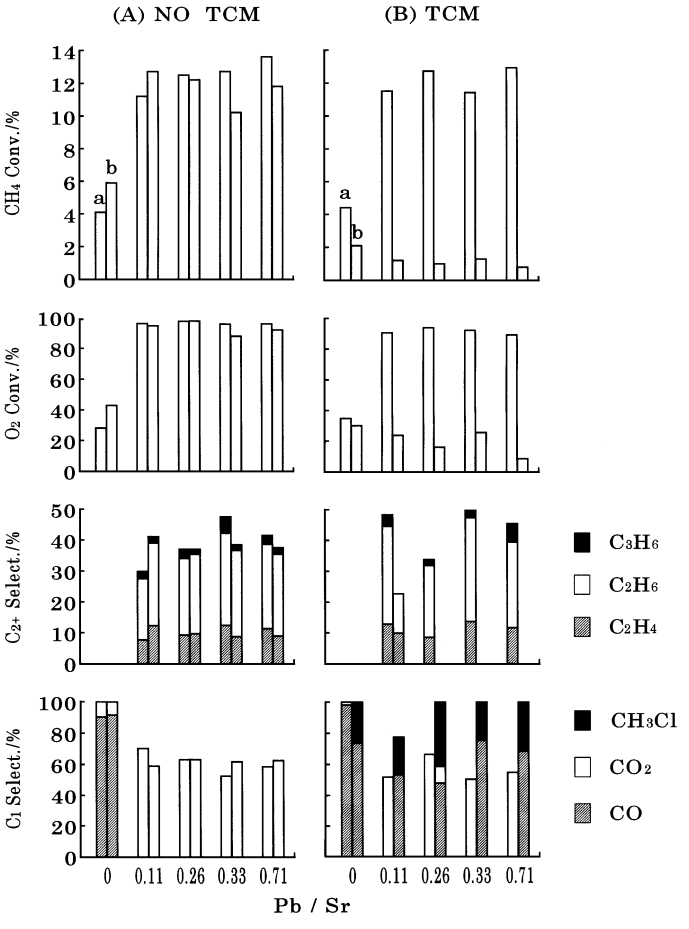

FIG. 2. Methane oxidation on SrHAp and various SrPbHAp in the presence and absence of TCM at 873 K. Conditions: $W = 0.5$ g, $F = 30$ mL/min, $P(CH_4) = 28.7$ kPa, $P(O_2) = 4.1$ kPa, and $P(TCM) = 0.17$ kPa (when present) diluted with He. Catalysts were pretreated with O_2 (25 mL/min) at 873 K for 1 h. Symbols: a, 0.5 h on-stream: b, 6 h on-stream.

of the catalysts were completely converted to the corresponding chlorapatite, $Sr_{10}(PO_4)_6Cl_2$ [JCPDS 16-0666] and $Pb_{10}(PO_4)_6Cl_2$ [JCPDS 19-0701], except that of SrPb11HAp, in which a small amount of $Sr_3(PO_4)_2$ was still evident. As noted from Fig. 2, reaction results which were obtained in the presence of TCM at 6 h on-stream from SrPb11HAp were distinctly different from those found with the remaining catalysts. In particular C_2 hydrocarbons were observed with SrPb11HAp which were absent under these conditions with the remaining catalysts, apparently due to the presence of $Sr_3(PO_4)_2$ in the former material. Since no phosphates were detected in the XRD of SrPb33HAp and SrPb71HAp which had been previously employed in the oxidation in the presence of TCM, the phosphates formed during the pretreatment have evidently been converted to the corresponding chlorapatites from the corresponding hydroxyapatites the latter of which had been reconverted during the oxidation process. In the XPS spectra of samples previously employed in obtaining the results reported in

TABLE 3

Surface Area of SrHAp and SrPbHAp Catalysts Previously Employed in the Oxidation in the Presence and Absence of TCM at 773 and 873 K Reaction Temperatures and Specific Activities at 0.5 and 6 h On-Stream

	Surface area[a]				Specific activity[b]							
	773 K		873 K		773 K				873 K			
	A[c]	P[c]	A	P	A		P		A		P	
	6	6	6	6	0.5	6	0.5	6	0.5	6	0.5	6
SrHAp	51.6	22.5	29.8	21.9	0.7	0.2	0.6	3.4	7.9	25.0	8.5	12.1
SrPb11HAp	43.3	18.5	22.3	10.2	2.5	4.7	2.1	6.8	25.4	72.0	26.4	14.9
SrPb26HAp	20.2	13.7	9.0	10.5	17.6	18.8	11.9	7.8	70.9	171.5	73.0	12.1
SrPb33HAp	32.6	15.5	8.9	4.8	9.5	14.7	8.7	4.9	34.4	143.5	30.9	34.3
SrPb71HAp	15.5	5.6	3.4	2.4	28.5	31.0	26.3	9.0	99.4	439.0	94.3	42.2

[a] In m^2/g. In Catalysts previously employed in obtaining the results shown Figs. 2 and 4 but after 0.5 and 6 h on-stream.

[b] 10^{-6} mmol/s · m^2. Specific activities at 0.5 and 6 h were calculated with using the surface area of fresh catalysts and those used in the oxidation after 6 h on-stream, respectively.

[c] A, absence of TCM; P, presence of TCM.

Fig. 3B, peaks attributed to Sr $3p_{1/2}$, Sr $3p_{3/2}$, O 1s, P 2s, and Pb $4f_{5/2}$ (when present) were found at approximately 280, 270, 532, 191, and 144 eV either before or after argon-ion etching (Fig. 4), all of which were also found in the fresh catalysts. Furthermore the peak due to Cl 2p was also detected at approximately 199 eV in the previously employed samples (Fig. 4). In some catalysts, the peak due to the metallic state of lead (Pb^0) was also found at approximately

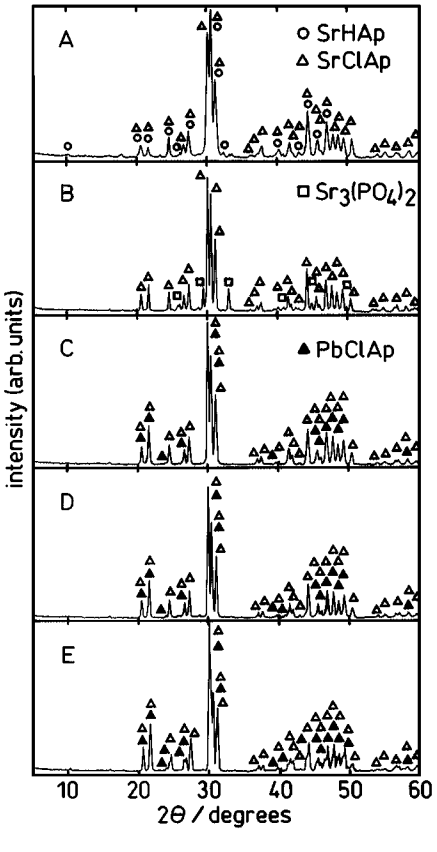

FIG. 3. XRD patterns of catalysts previously employed in obtaining the results shown in Fig. 2B. Symbols are as in Fig. 1.

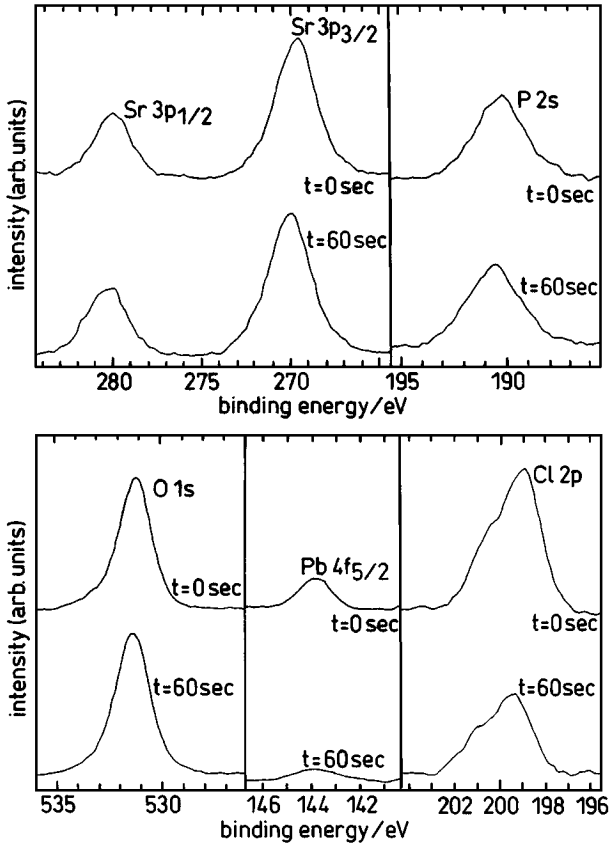

FIG. 4. XPS spectra of SrPb11HAp previously employed in obtaining the results reported in Fig. 3B. *t*, etching time.

TABLE 4

XPS Analyses of Fresh Catalysts and Used[a] in the Presence of TCM

		Sr/P[c]			Pb/P[c]			Cl/P[c]			Cl/P[d]
					Temperature[e]						
Catalyst	T^b	F	773	873	F	773	873	F	773	873	773
SrHAp	0	1.64	1.65	1.79	—	—	—	—	0.62	0.58	0.64
	1	1.92	1.80	1.84	—	—	—	—	0.57	0.55	
SrPb11HAp	0	1.46	1.68	1.75	0.21	0.13	0.16	—	0.54	0.60	0.53
	1	1.78	1.77	1.91	0.04	0.07	0.08	—	0.40	0.37	
SrPb26HAp	0	1.11	1.41	1.46	0.70	0.30	0.35	—	0.57	0.49	0.54
	1	1.38	1.48	1.48	0.28	0.15	0.17	—	0.32	0.33	
					(0.10	0.19	0.17)[f]				
SrPb33HAp	0	1.34	1.25	1.37	0.51	0.36	0.36	—	0.49	0.46	0.49
	1	1.47	1.43	1.62	0.21	0.09	0.19	—	0.36	0.30	
					(0.16	0.21	0.24)[f]				
SrPb71HAp	0	1.08	1.03	1.18	0.66	0.51	0.40	—	0.48	0.41	0.54
	1	1.39	1.45	1.40	0.19	0.15	0.27	—	0.39	0.27	
					(—	0.25	0.18)[f]				

[a] Previously employed in obtaining the results reported in Fig. 2B or 4B, but after 6 h on-stream.
[b] Etching time (min).
[c] Atomic ratio determined with XPS.
[d] Atomic ratio in bulk phase.
[e] Reaction and pretreatment temperatures (K); "F" refers to the fresh catalyst.
[f] Atomic ratio of Pb^0/Pb^{2+}.

142 eV as shown in Table 4. The Sr/P ratios found before and after the oxidation process in the presence of TCM at 873 K showed relatively small differences for a given catalyst. In contrast, the values of Pb/P found with the used samples show clearly evident decreases in comparison with those found on the corresponding fresh catalysts and the values of this ratio in the bulk of the used samples are considerably smaller than those in the surface region, indicative both of the loss of Pb from the surface region of the catalysts and the conversion of Pb^{2+} to the metallic Pb^0 during the oxidation, the latter of which may be due to the presence of oxidation products, for example, CO and H_2, which are themselves capable of participating in the reduction of lead. The relatively large values obtained for Pb^0/Pb^{2+} (Table 4) suggest that the metallic lead is largely retained on and in the catalysts, consistent with the absence of any visual evidence for the vaporization and subsequent downstream deposition of the metal (46). No obvious correlation of the Cl/P ratio in the near-surface region with the lead content of the catalysts was found, but the surface-enhanced concentration of chlorine is evident, particularly with those catalysts containing lead.

Figure 5 shows the effects of the addition of small partial pressures of TCM into the feedstream at the reaction and pretreatment temperatures of 773 K, at which all of the catalysts are present relatively stably as the hydroxyapatite (Table 2). At this temperature no C_2 hydrocarbons are formed regardless of the lead content and the addition of TCM. In the absence of TCM (Fig. 5A), the conversion of methane and the selectivity to CO_2 increased with the lead content, indicating a lead-induced enhancement of the deep oxidation of methane. The specific activities also increased with lead content, although not in an entirely continuous manner, but no correlation is evident for its changes with time-on-stream (Table 3). In the presence of TCM (Fig. 5B), the formation of methyl chloride was observed after 6 h on-stream, but not after 0.5 h on-stream, with both the lead-free and the SrHAp ion-exchanged with lead. The conversion of methane increased with lead content for time-on-stream of 0.5 h, while passing through a maximum for 6 h on-stream. The selectivity to CH_3Cl increased to 73% for SrPbHAp with Pb/Sr equal to 0.26 and remained relatively unchanged for higher lead contents. It is noteworthy that the introduction of TCM with calcium and strontium hydroxyapatites has been shown to result in an enhanced selectivity to CO (30–34). The XRD analyses showed that all of the catalysts after the reaction in the presence of TCM (Fig. 5) were converted to the corresponding chlorapatites, and no phosphates were observed with any of the catalysts. The XPS spectra of the catalysts previously employed in the presence of TCM at 773 K showed the peaks found for those at 873 K (Table 4). The atomic ratios of Sr/P, Pb/P, and Cl/P, together with Pb^0/Pb^{2+}, in the near-surface region of the catalysts used at 773 K were little different from those used at 873 K. The atomic ratios of Cl/P in the bulk phase of SrHAp, SrPb11HAp, SrPb26HAp, SrPb33HAp, and SrPb71HAp were essentially identical to those

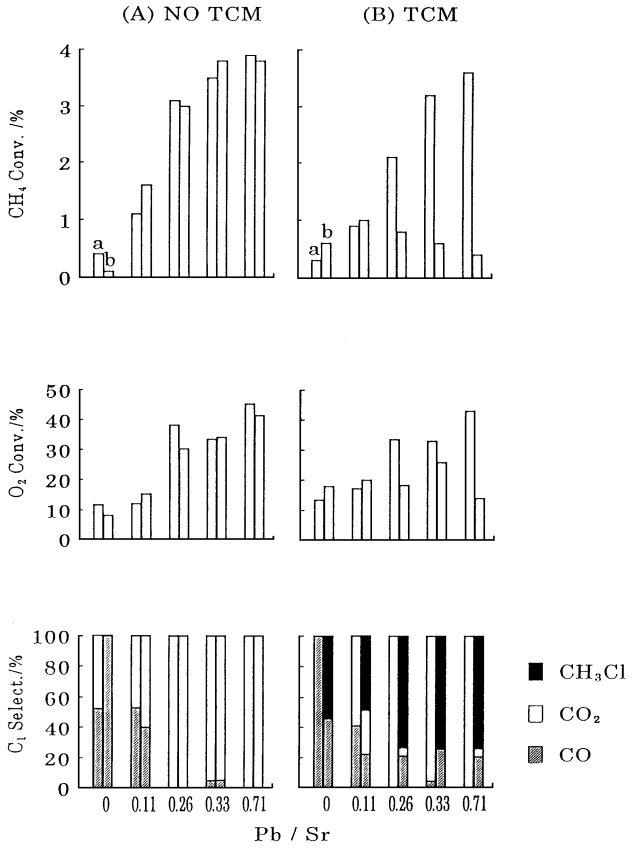

FIG. 5. Methane oxidation on SrHAp and various SrPbHAp in the presence and absence of TCM at 773 K. Conditions and symbols are as in Fig. 2, except for the pretreatment and reaction temperatures (both 773 K).

estimated by XPS (Table 4), indicating that other chlorinated species together with the chlorapatite were formed in and on the catalysts during the oxidation with TCM since the theoretical ratio of Cl/P for each corresponding apatite is 0.33. It is interest to note that etching results in a surface composition similar to that expected for chlorapatite, indicative of the removal of chlorinated species by the etching or surface enhancement of chlorine (46).

Effects of the Fine Structure Changes of the Catalysts on the Methane Oxidation

It is generally accepted that the active sites in the oxidation of methane on solid catalysts contain oxygen in some form, although not to exclude the presence of other elements, and the activity is also strongly influenced by the electronegativity of the cations. In the SrHAp and SrPbHAp systems, it is expected that Sr and/or Pb cations would exert a perturbing influence on the oxygen species and in particular the Sr–O and/or Pb–O bond distances which may, in turn, alter the electronegativities of the oxygen species. Therefore EXAFS analyses were applied to provide information on the bond distances and the environment of the Sr and/or Pb atoms. Although EXAFS

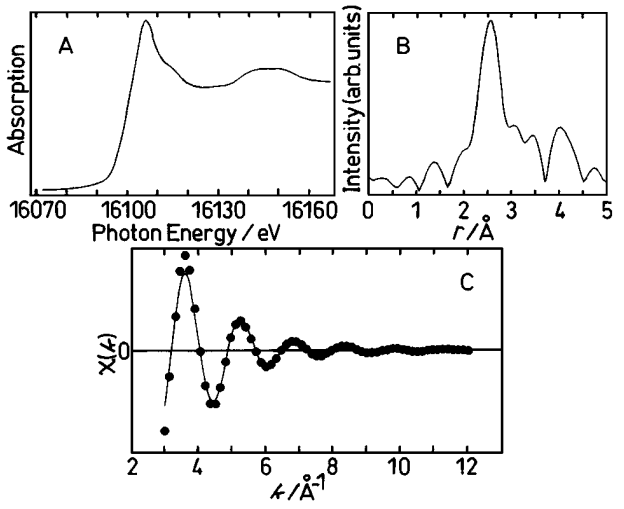

FIG. 6. XANES spectra (A), Fourier transformation of k^3-weighted EXAFS oscillation (B), and the curve-fitting near Sr K-edge (C) measured at 300 K of the fresh SrPb26HAp calcined at 773 K. Solid line in (C), experimental data; closed circles in (C), calculated values.

analyses provide information only on bulk phases, the properties of the surface of each apatite on which the catalysis occurs are undoubtedly strongly influenced by those of the bulk phase. The X-ray absorption near-edge structure (XANES) spectra near the Sr K-edge and Pb L_3-edge of the fresh SrPb26HAp are shown in Figs. 6A and 7A, respectively. The shape of the XANES spectra and the edge positions of each catalyst near the Sr K-edge and Pb L_3-edge were similar (not shown), indicating that the electronic configuration and site symmetry of the strontium and lead in each catalyst are not significantly different. Figures 6B and 7B show the Fourier transforms of the EXAFS oscillation around the Sr K-edge and Pb L_3-edge

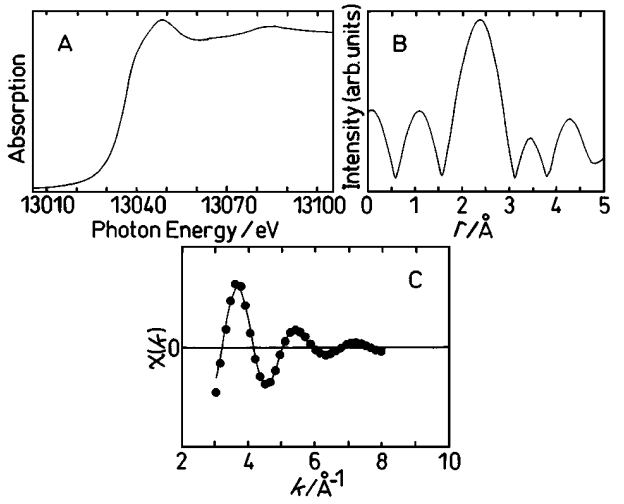

FIG. 7. XANES spectra (A), Fourier transformation of k^3-weighted EXAFS oscillation (B) and the curve-fitting near Pb L_3-edge (C) measured at 300 K of the fresh SrPb26HAp calcined at 773 K. Symbols are as in Fig. 5.

TABLE 5

Results of Curve-Fitting Analyses for Fresh Catalysts[a]

Catalyst	r_{Sr-O}[b]/Å	r_{Pb-O}[b]/Å	N[c]	σ[d]/Å^2	E_0[e]/eV	R[f] (%)
SrHAp	2.52	—	5.6	0.102	3.92	15.6
SrPb11Hap	2.51	—	5.5	0.101	3.59	14.9
SrPb26HAp	2.52	—	5.9	0.102	4.19	15.0
SrPb33HAp	2.52	—	5.8	0.103	3.90	15.0
SrPb71HAp	2.52	—	5.8	0.101	4.36	14.0
SrPb11HAp	—	2.27	4.4	0.149	6.94	12.2
SrPb26HAp	—	2.31	4.4	0.151	7.72	14.5
SrPb33HAp	—	2.30	4.4	0.151	7.65	15.3
SrPb71HAp	—	2.31	4.4	0.157	8.35	17.5

[a] Calcined at 773 K for 3 h in air.
[b] Distance; estimated maximum deviation (±0.01).
[c] Coordination number; estimated maximum deviation (±1).
[d] Debye–Waller (like) factor.
[e] Reliability factor.

of the fresh SrPb26HAp, respectively. Phase shifts are not corrected in these spectra. The strongest peak in each spectrum corresponds to the nearest-neighbor distance for Sr–O and Pb–O, respectively (43). The nearest-neighbor Pb–O and/or Sr–O distances of each fresh catalyst are anticipated to have the strongest relationship to the catalytic activities (32). Thus, the reliability of the phase shift and amplitude functions are tested at approximately the nearest distance by fitting the observed EXAFS of each fresh catalyst. Figures 6C and 7C show the optimum curve fitting around the Sr K-edge and Pb L_3-edge of the fresh SrPb26HAp, in which solid lines represent the experimental data and the closed circles represent the calculated results. The results of the curve fitting analyses for all fresh catalysts are described in Table 5. Although the nearest-neighbor distances of the Sr–O bond of each catalyst are independent of the lead content and are virtually identical, that of the Pb–O of SrPb11HAp is shorter than those of the remaining leaded catalysts. Comparison of the bond distances of Sr–O and Pb–O with the conversion of methane in the absence of TCM on each catalyst at 773 K (Fig. 5A) reveals that the conversion on SrPb11HAp was higher than that on SrHAp while smaller than that on the remaining leaded catalysts, the latter of which have similar activity in the oxidation of methane in the absence of TCM. Furthermore, comparison of the bond distances of Pb–O with the specific activities in the absence of TCM at 773 K (Table 3) reveals that, with the exception of SrPb26HAp, the specific activities increased with increasing Pb–O bond distances. Therefore it appears that the conversion of methane is strongly influenced by the nearest-distance of Pb–O but not Sr–O. Similar correlations between, conversions, activities and selectivities and the bond distances determined with EXAFS have been reported in our previous papers on the oxidation of methane on calcium hydroxyapatites and those doped with lead (32, 47).

Active Sites for the Oxidation of Methane on SrHAp and SrPbHAp

In the present section, active sites for the oxidation of methane at 773 K, at which temperatures the catalysts are thermally stable are discussed together with the role of TCM in the oxidation process.

In the absence of TCM, it is evident that the activities of the catalysts increase with increasing lead content up to a Pb/Sr ratio of 0.33 (Fig. 5). The nearest bond distances of Pb–O increase on increase of the Pb/Sr ratio from 0.11 to 0.26 but remain approximately constant for further increases in the lead content, while the corresponding Sr–O distances show little or no differences between the various catalysts (Table 5). Similar relationships are also evident with the specific activities. Therefore the observed increases in activity appear to be more closely related to the Pb–O distances rather than those of Sr–O and consequently the oxygen species in proximity to the lead cations are predominantly involved in the C–H bond scission. Asami *et al.* (8), working with MgO- and Al_2O_3-supported lead oxide catalysts earlier concluded that the lattice oxygen of PbO is the active species in the oxidative coupling reaction. Since the activities of the calcium (30–32), strontium (33, 34), and the present strontium–lead hydroxyapatites decrease with increasing time-on-stream in the presence of TCM, apparently as a result of the formation of the corresponding chlorapatites, hydroxyl groups must also participate in the methane activation process.

Earlier work on a variety of catalysts found that the introduction of TCM to the feedstream for the partial oxidation of methane generally produced enhanced selectivities to CO while with the oxidative coupling the selectivities to C_{2+} hydrocarbons, particularly ethylene, were increased (29). However, studies employing heteropoly oxometalates in the partial oxidation process, particularly the strongly acidic 12-tungstophosphoric acid, found high selectivities to methyl chloride (48, 49). As shown in the present work, the results obtained with strontium hydroxyapatite with and without ion-exchanged lead are markedly dissimilar from those found with calcium hydroxyapatite and the majority of catalysts when employed in the presence of TCM. The formation of CH_3Cl at longer times-on-stream but its absence at 0.5 h on-stream on strontium hydroxyapatite either with or without ion-exchanged lead indicates that the process through which CH_3Cl is formed is a two-phase process, presumably involving the catalytic surface and in particular that which contains some critical concentration of chloride. Although the XRD patterns demonstrate that at least a substantial portion of the chloride exists as the chlorapatite, it is nevertheless possible that the surface, and the bulk as well, contain chlorine in positions other than those previously occupied by the hydroxyl groups of the apatite. Indeed the atomic ratios of Cl/P in the surface and bulk phases of each used catalyst are larger than the theoretical

ratio (0.33). While there is evidence for the participation of the lead in the ion-exchanged catalyst in the selective production of CH_3Cl it is however clear that the formation of the chloromethane does not require the presence of this element and it is, of course, conceivable that its involvement is more indirect than direct. The XPS data suggest that some reduction of the lead cations occurs during the oxidation process and there is evidence that the presence of TCM contributes to this reduction process (31). Evidence for the existence of a redox cycle between Pb^0 and Pb^{2+} species has been reported earlier with supported lead oxide catalysts (8). The roles of ion-exchanged lead and TCM and their possible interactive participation in the production of CH_3Cl remain to be clarified.

CONCLUSIONS

(i) The thermal stability of the apatites is generally reduced by the introduction of lead. The conversion of the apatites to the corresponding phosphates was observed in SrPb11HAp, SrPb22HAp and SrPb71HAp at 873 K while the apatite structure was retained in SrHAp and SrPb26HAp at the same temperature.

(ii) At 873 K, in the absence of TCM, the conversion of methane, the selectivities to C_2, particularly ethane, and to CO increased with the introduction of small quantities of lead but were relatively unchanged with further additions of this element. The specific activities generally increased with the content of lead, although not uniformly, and also increased with time-on-stream, the latter largely due to the substantial decreases in surface area.

(iii) At 873 K in the presence of TCM, the addition of lead to the catalysts resulted in significant reductions of the conversion and the selectivity to C_2 hydrocarbons together with the increase of that to CO, particularly at the higher times-on-stream. However, no particular trend was evident for the specific activities with time-on-stream among the various compositions. The corresponding chlorapatites were formed in the catalysts used in the presence of TCM.

(iv) At 773 K, in the absence of TCM, the conversion of methane and the specific activities (with the exception of that for SrPb26HAp) increased with increasing lead content, apparently relating to the nearest-neighbor distance of the Pb–O bond as estimated from EXAFS. No C_2 compounds were obtained at this temperature but lead enhanced the deep oxidation to CO_2.

(v) At 773 K in the presence of TCM no CH_3Cl was observed at 0.5 h time-on-stream with strontium hydroxyapatites either with or without ion-exchanged lead. However, at 6 h time-on-stream selectivities to CH_3Cl as high as 73% were observed with SrPb26HAp. The formation of the chlorapatites was again confirmed in the catalysts employed in the oxidation process in the presence of TCM.

ACKNOWLEDGMENTS

This work was partially funded by a "Grant for Natural Gas Research" of The Japan Petroleum Institute to S.S. and the Natural Sciences and Engineering Research Council of Canada to J.B.M. and was supported by the Satellite Venture Business Laboratory, "Nitride Photonic Semiconductor Laboratory" of The University of Tokushima, to which our thanks are due. This work has been performed under the approval of the Photon Factory Program Advisory Committee (Proposal No. 95G193).

REFERENCES

1. Hinsen, W., Bytyn, W., and Baerns, M., *in* "Proceedings, 8th International Congress Catalysis, Berlin, 1984," Vol. 3, p. 581. Verlag Chemie, Weinheim, 1984.
2. Otsuka, K., Jinno, K., and Morikawa, A., *Chem. Lett.* 499 (1985).
3. Sinev, M. Y., Vorob'eva, G. A., and Kornak, U. N., *Kinet. Katal.* **27**, 1007 (1986).
4. Bytyn, W., and Baerns, M., *Appl. Catal.* **28**, 199 (1986).
5. Grzybek, T., and Baerns, M., *J. Catal.* **129**, 106 (1991).
6. Asami, K., Hashimoto, S., Shikada, T., Fujimoto, K., and Tominaga, H., *Ind. Eng. Chem. Res.* **26**, 1485 (1987).
7. Roos, J. A., Bakker, A. G., Bosch, H., van Ommen, J. C., and Ross, J. R. H., *Catal. Today* **1**, 133 (1987).
8. Asami, K., Shikada, T., Fujimoto, K., and Tominaga, H., *Ind. Eng. Chem. Res.* **26**, 2348 (1987).
9. Carreiro, J. A. S. P., Follmer, G., Lehman, L., and Baerns, M., *in* "Proceedings, 9th International Congress on Catalysis, Calgary, 1988" (M. J. Phillips and P. Ternan, Eds.), Vol. 2, p. 891. Chem. Inst. of Canada, Ottawa, 1988.
10. Aika, K., and Nishiyama, T., *in* "Proceedings, 9th International Congress on Catalysis Calgary, 1988" (M. J. Phillips and M. Ternam, Eds.), Vol. 2, p. 907. Chem. Inst. of Canada, Ottawa, 1988.
11. Bartek, J. P., Hupp, J. M., Brazdil, J. F., and Grasselli, R. G., *Catal. Today* **3**, 117 (1988).
12. Thomas, J. M., Ueda, W., Williams, J., and Harris, K. D. M., *Faraday Discuss. Chem. Soc.* **87**, 33 (1989).
13. Kharas, K. C. C., and Lunsford, J. H., *J. Am. Chem. Soc.* **111**, 2336 (1989).
14. Fujimoto, K., Hashimoto, S., Asami, K., Omata, K., and Tominaga, H., *Appl. Catal.* **50**, 223 (1989).
15. Agarwal, S. K., Migone, R. A., and Marcelin, G., *J. Catal.* **121**, 110 (1990).
16. Agarwal, S. K., Migone, R. A., and Marcelin, G., *J. Catal.* **123**, 228 (1990).
17. Sinev, M. Y., Bychkov, V. Y., Korchak, V. N., and Krilov, O. V., *Catal. Today* **6**, 543 (1990).
18. Aika, K., Fujimoto, N., Kobayashi, M., and Iwamatsu, E., *J. Catal.* **127**, 1 (1991).
19. Smith, K. J., Painter, T. M., and Galuszka, J., *Catal. Lett.* **11**, 301 (1991).
20. Park, S.-E., and Chang, J.-S., *Appl. Catal. A* **85**, 117 (1992).
21. Mariscal, R., Soria, J., Pena, M. A., and Fierro, J. L. G., *Appl. Catal. A* **111**, 79 (1994).
22. Chang, J. S., and Park, S.-E., *Bull. Korean Chem. Soc.* **16**, 1148 (1995).
23. Amenomiya, A., Birss, V. I., Goledzinowski, M., Galuszka, J., and Sanger, A. R., *Catal. Rev.-Sci. Eng.* **32**, 163 (1990).
24. Carreiro, J. A. S. P., and Baerns, M., *React. Kinet. Catal. Lett.* **35**, 49 (1987).
25. Ohno, T., and Moffat, J. B., *Catal. Lett.* **16**, 181 (1992).
26. Matsumura, Y., and Moffat, J. B., *Catal. Lett.* **17**, 197 (1993).
27. Matsumura, Y., Moffat, J. B., Sugiyama, S., Hayashi, H., Shigemoto, N., and Saitoh, K., *J. Chem. Soc., Faraday Trans.* **90**, 2133 (1994).
28. Matsumura, Y., and Moffat, J. B., *J. Catal.* **148**, 323 (1994).
29. Moffat, J. B., Sugiyama, S., and Hayashi, H., *Catal. Today* **37**, 15 (1997).

30. Sugiyama, S., Minami, T., Hayashi, H., Tanaka, M., Shigemoto, N., and Moffat, J. B., *J. Chem. Soc. Faraday Trans.* **92**, 293 (1996).
31. Sugiyama, S., Minami, T., Hayashi, H., Tanaka, M., Shigemoto, N., and Moffat, J. B., *Energy Fuels* **10**, 828 (1996).
32. Sugiyama, S., Minami, T., Moriga, T., Hayashi, H., Koto, K., Tanaka, M., and Moffat, J. B., *J. Mater. Chem.* **6**, 459 (1996).
33. Sugiyama, S., Minami, T., Hayashi, H., Tanaka, M., and Moffat, J. B., *J. Solid State Chem.* **126**, 242 (1996).
34. Sugiyama, S., Minami, T., Higaki, T., Hayashi, H., and Moffat, J. B., *Ind. Eng. Chem. Res.* **36**, 328 (1997).
35. Kreidler, E. R., and Hummel, F. A., *Am. Mineral.* **55**, 170 (1970).
36. Bett, J. A. S., Christner, L. G., and Hall, W. K., *J. Catal.* **13**, 332 (1969).
37. Kibby, C. L., and Hall, W. K., *J. Catal.* **29**, 144 (1973).
38. Kibby, C. L., and Hall, W. K., *J. Catal.* **31**, 65 (1973).
39. Monma, H., *J. Catal.* **75**, 200 (1982).
40. Imizu, Y., Kadoya, M., and Abe, H., *Chem. Lett.* 415 (1982).
41. Izumi, Y., Sato, S., and Urabe, K., *Chem. Lett.* 1649 (1983).
42. Matsumura, Y., Sugiyama, S., Hayashi, H., Shigemoto, N., Soitoh, K., and Moffat, J. B., *J. Mol. Catal.* **92**, 81 (1994).
43. Sugiyama, S., Moriga, T., Goda, M., Hayashi, H., and Moffat, J. B., *J. Chem. Soc., Faraday Trans.* **92**, 4305 (1996).
44. McKale, A. G., Veal, B. W., Paulikas, A. P., Chan, S. K., and Knapp, G. S., *J. Am. Chem. Soc.* **110**, 3763 (1988).
45. Sakane, H., Miyanaga, T., Watanabe, I., Matsubayashi, N., Ikeda, S., and Yokoyama, Y., *Jpn. J. Appl. Phys.* **32**(1), 4641 (1993).
46. We thank the referees for drawing our attention to this point.
47. Sugiyama, S., Minami, T., Moriga, T., Hayashi, H., and Moffat, J. B., *J. Solid State Chem.* [In press]
48. Ahmed, S., and Moffat, J. B., *Catal. Lett.* **1**, 141 (1988).
49. Ahmed, S., and Moffat, J. B., *J. Catal.* **118**, 281 (1989).